AIP Advances

Magnetotransport and thermal properties characterization of 55 K superconductor SmFeAsO0.85F0.15

Amit Srivastava, Anand Pal, Saurabh Singh, C. Shekhar, H. K. Singh, V. P. S. Awana, and O. N. Srivastava

Citation: AIP Advances **3**, 092113 (2013); doi: 10.1063/1.4821335
View online: http://dx.doi.org/10.1063/1.4821335
View Table of Contents: http://scitation.aip.org/content/aip/journal/adva/3/9?ver=pdfcov
Published by the AIP Publishing

Magnetotransport and thermal properties characterization of 55 K superconductor $SmFeAsO_{0.85}F_{0.15}$

Amit Srivastava,[1] Anand Pal,[2] Saurabh Singh,[1] C. Shekhar,[3] H. K. Singh,[2] V. P. S. Awana,[2,a] and O. N. Srivastava[1]

[1]*Nano Science and Nanotechnology Centre, Department of Physics, Banaras Hindu University, Varanasi, U.P. 221005, India*

[2]*Quantum Phenomena and Application Division, National Physical Laboratory (CSIR), Dr. K. S. Krishnan Road, New Delhi-110012, India*

[3]*Max Plank Institute for Chemical Physics of Solids, Dresden-01187 Germany*

(Received 12 June 2013; accepted 21 August 2013; published online 10 September 2013)

This report fairly underlines the magneto-transport, thermal properties characterization and bulk superconductivity in the FeAs-based $SmFeAsO_{0.85}F_{0.1}$. The phase formation and structure are confirmed by Rietveld analysis of room temperature powder X-ray diffraction (*XRD*) data. Electron microscopy was employed to unravel the micro structural details, such as perfection of the lattice and the grain morphology including size and boundaries. The electrical and magnetic measurements have been carried out to confirm the bulk superconductivity and understand the nature of electrical transport in the normal and superconducting state. The intra-grain critical current density (J_c) with applied magnetic field is calculated from isothermal *DC* magnetization (*MH*) plots using conventional Bean critical state model. Superconductivity is observed at transition temperature (T_c) above 55 K without *HPHT* (high pressure high temperature) synthesis route. The value of J_c is found to be around 5.26 $\times$ 10^4 A/cm^2 at 5 K in zero field. The dependence of thermally activated flux flow energy (U/k_B) on the applied magnetic field has been observed. *AC* susceptibility measurements were performed for 55 K superconducting $SmFeAsO_{0.85}F_{0.15}$ sample at various amplitude of applied *AC* drive field and its granular nature is confirmed. The parent compound SmFeAsO is found to be magnetic with Fe spin density wave (*SDW*) like order below 150 K, on the other hand the F doped $SmFeAsO_{0.85}F_{0.15}$ sample is bulk superconducting at below 55 K. Both Fe (*SDW*) at 150 K for SmFeAsO and 55 K superconductivity in case of $SmFeAsO_{0.85}F_{0.15}$ sample has confirmed by Specific heat [$C_p(T)$] measurement too. Further Sm orders anti-ferro-magnetically at 4.5 K for non-superconducting and at 3.5 K for superconducting samples, also the entropy change is reduced significantly for the later than the former. Summarily complete physical property characterization for both non-superconducting SmFeAsO and 55 K superconductor $SmFeAsO_{0.85}F_{0.15}$ samples is provided and discussed in the current article. [http://dx.doi.org/10.1063/1.4821335]

I. INTRODUCTION

The discovery of the new class of oxypnictide superconductors including iron-based $LaFeAsO_{1-x}F_x$ with critical temperature T_c at 26 K[1] has provided new impetus to research in the area of high-temperature superconductivity, and has resulted in unravelling of several new issues in the domain of high temperature superconductivity in materials incorporating Fe-As layers as the critical structural unit.[2–8] Such newfangled materials have the general formula REFeAsO, where RE

[a]Corresponding author's email: awana@mail.nplindia.ernet.in. Fax No. +91-11-45609310: Phone no. +91-11-45609357. Web page- www.freewebs.com/vpsawana/

is a rare earth element. The structural unit consists of alternating RE-O and Fe-As layers, rendering charge carriers and conducting planes, respectively. In fact these new systems are structurally similar to HTSc cuprates. Though both the Cuprates and the Fe-pnictides are layered superconductors having superconductivity in CuO_2 planes and FeAs layers respectively, the Fe-pnictides are known to be less anisotropic than the Cuprates. Primarily due to the reason, that the unit cells of Fe-pnictides are more compact in comparison to HTSc cuprates. The Fe pnictides have only one redox layer (RE-O) adjacent to FeAs superconducting layer in c-direction. However in case of cuprates the unit cells are larger and the superconducting CuO_2 planes are sandwiched between more than one non superconducting block and hence are relatively more anisotropic than the Fe-pnictides. The T_c in this class of materials generally depends on (i) the size of the RE^{3+} ions, (ii) F substitution on oxygen sites, and (iii) oxygen deficiency in F-free materials. Several reports have shown that T_c can be effectively increased to above 55 K by substitution of larger La^{3+} ion with RE^{+} cations having smaller radii such as Ce, Pr, Nd, Sm, etc.[2–8] The un-doped (F free) REFeAsO compounds are non-superconducting and show a crystallographic phase transition around 150 K along with a static spin density wave (*SDW*) like long range ordering of the Fe spins below nearly the same temperature. The near concomitant structural and the magnetic transitions are confirmed by an anomaly, which is generally seen as a sharp metallic step at around 150 K in the temperature dependence of resistivity (ρ - T) and also by the hump around the same temperature in the heat capacity.[1–10] Introduction of carriers is observed to shift the spin density wave and the structural phase transition temperatures to lower temperature values and superconductivity appears with disappearance of both the *SDW* and the structural phase transitions. The Fe spin density wave (*SDW*) like order at $T < 150$ K happens in case of non superconducting ground state REFeAsO. Superconductivity appears with carrier doping from REO layer and the *SDW* order of Fe spins disappears. The exact nature of Fe spins *SDW* ordering is established from neutron scattering and Mossbauer spectroscopy studies.[4–6,10]

In the REFeAsO system, positively charged RE-O layers that sandwich negatively charged Fe-As layers along the *c*-axis, act as an insulating charge reservoir layer, while the Fe-As layer acts as a active block responsible for the conduction mechanism in these compounds and is usually referred to as the superconducting layer.[1–7,9] Superconductivity can be induced by (i) F substitution at O sites in RE-O layer[1–9] and (ii) substitution of 3d metals like Co and Ni at Fe sites.[11,12] The T_c of the 3d metal substituted compounds is generally found to be lower and is believed to be due to the enhanced impurity scattering and pair breaking in the conduction layers. In contrast, the F substitution shows the highest T_c of up to 55 K. The upper critical field (Hc_2) is observed to increase appreciably with lowering of the RE cationic size. For example it has been estimated that $Hc_2 \sim$ 63–65T for $LaFeAsO_{0.9}F_{0.1}$, $Hc_2 \sim$ 70T for $PrFeAsO_{0.85}F_{0.15,}$ 230T for high-pressure fabricated $NdFeAsO_{0.82}F_{0.18}$ and for $SmFeAsO_{0.85}F_{0.15,}$ it is over 200T.[13–16] Thus Sm substituted compounds can be highly useful in high current/field applications. The tremendous interest in these compounds is not only due to their high critical temperatures, high upper critical fields, and the ability to sustain high current densities at elevated temperatures but also due to the intriguing presence of well-known magnetic iron (Fe) element in the superconducting Fe-As plane. The micro-structural aspects of the Fe-As and RE-O layers and their impact on the superconducting properties are not very well understood yet.

The current article deals with the emergence of superconductivity in F-substituted $SmFeAsO_{0.85}F_{0.15}$ with $T_c \sim 56$ K, which is the highest to the best of our knowledge for bulk samples prepared by normal two-step synthesis method at low temperature and without invoking high *HPHT*. The previous works have reported such high T_c values in excess of ~55 K, with *HPHT* synthesis process.[8,17] We have studied the correlation between the micro-structural properties and superconducting characteristics such as the T_c and the critical current density (J_c) along with the flux pinning behaviour of the bulk samples synthesised at low temperature by a two-step solid state reaction route.

II. EXPERIMENTAL DETAILS

Polycrystalline bulk samples with nominal composition $SmO_{1-x}F_xFeAs$ (x = 0.0 and 0.15) were synthesized by conventional solid state sintering method using high-purity As, Fe, SmF_3 and

Sm_2O_3 powders all with high purity from Sigma Aldrich as starting materials. To obtain SmAs-Fe_2As-FeAs powder, Sm, Fe and As were weighed according to the stoichiometric ratio of 1:3:3, mixed and ground thoroughly using mortar and pestle under high purity Ar atmosphere in glove box. The humidity and oxygen content in the glove box was maintained to be less than 1ppm. The mixed powder was pelletized in disk shape and then encapsulated in an evacuated (10^{-3} Torr) silica tube. Then the silica tube embodying the said pellet was heat treated for 12 hrs at 800 °C. Further, in the next step, SmAs, Fe_2As and FeAs were mixed with dehydrated Sm_2O_3, Sm and SmF_3 in accordance with $(1 + x)$ Sm + $(1 - x)$ Sm_2O_3 + $xSmF_3$ + 3FeAs stoichiometric ratio, where $x = 0$ for undoped and 0.15 for fluorine doped sample, was compacted and finally heated at 950° C for 72 hrs in continuum with slow heating rate to obtain a sintered pellet. To prevent silica tube from collapsing during the reaction, the tube was filled with high purity Ar gas. The furnace was then allowed to cool in a natural way. The sintered sample was obtained by breaking the quartz tube. The as sintered sample is concrete ceramic-like with dark-coloured surface.

Phase identification and crystal structure investigation were carried out by using powder *X*-ray diffraction (*XRD*) with Philips X'PERT, PRO PAN Analytical X-ray diffractometer with Cu-Kα irradiation (wavelength, $\lambda = 1.5406$ Å) at a scanning speed of 0.02° s^{-1}. The lattice parameters derived from *X*-ray diffraction patterns were subjected to Rietveld refinement using the FULLPROF SUITE program. Microstructures of the samples under investigations and its morphology were studied using environmental scanning electron microscopy (*SEM*, Quanta 200), operated at 30 kV. Further studies to unravel the microstructure, microstructural characterization were carried out by high resolution transmission electron microscopy (*HRTEM*, *FEI* Tecnai 20G2 operated at 200 kV). The resistivity measurements were performed by a conventional four-point-probe method on a Quantum Design Physical Property Measurement System (*PPMS*-140kOe). Magnetic, transport and thermal properties of the samples were carried out with a Physical Property Measurement System (*PPMS*-Quantum Design) in the temperature range 2–300 K and in field up to 13Tesla.

III. RESULTS AND DISCUSSION

The typical *XRD* patterns of the as synthesized pristine SmFeAsO and F-doped $SmFeAsO_{0.85}F_{0.15}$ samples are shown in Fig. 1. The Rietveld refinement of X-ray diffraction data collected at room temperature confirmed that all observed reflections are indexed on the basis of tetragonal ZrCuSiAs-type structure with a space group *P*4/*nmm*. The simulated pattern shows that the studied samples are nearly single phase except for a weak impurity diffraction peak (marked with * in the *XRD* pattern) in the F-doped compound. These impurity peaks are assigned to the rare earth oxides. Based on the known structural details Sm and As are taken to be located at the Wyckoff position 2*c* (1/4, 1/4, *z*), the Fe at 2*b* (3/4, 1/4, 1/2), and the O/F are shared at site 2*a* (3/4, 1/4, 0). The lattice parameters obtained from the refinement are $a = 3.937(5)$ Å, $c = 8.509(6)$ Å and $a = 3.931(6)$ Å, $c = 8.474(1)$ Å for the pristine and 15% F-substituted samples, respectively. The smaller value of *c*-parameter in the F-substituted sample indicates a successful chemical substitution of F^{-1}($R_F = 1.33$ Å) at O^{2-} ($R_O = 1.40$ Å) site. These evaluated values of lattice parameters of the synthesized samples are close to those reported earlier,[3,13,14] which suggests successful synthesis of envisaged material. The observed structural results are quite consistent with the reports on other rare earth substitutions, and indicate the covalent character of the intra-layer chemical bonding due to the smaller covalent radius of fluorine than oxygen.

To understand the morphology and microstructure of the doped sample and their possible correlation with superconducting properties, *SEM* and *TEM* studies have been carried out on the same sample. Fig. 2(a) shows a representative scanning electron micrograph of $SmFeAsO_{0.85}F_{0.15}$ sample. The observation of the fractured specimen clearly shows the occurrence of layered structural units as the constituents of the polycrystalline bulk. This is consistent with the layered crystal structure of the compound. This type of feature has also been observed in high T_c cuprate superconductors. Since the grain boundaries in the samples are assumed to play a crucial role in determining the J_c and as it is strongly influenced by microstructure, extensive local area structural analysis has been done by employing *HRTEM*. In this approach, randomly selected grains have been examined and, during this course; it has been observed that there is an amorphous layer present around most

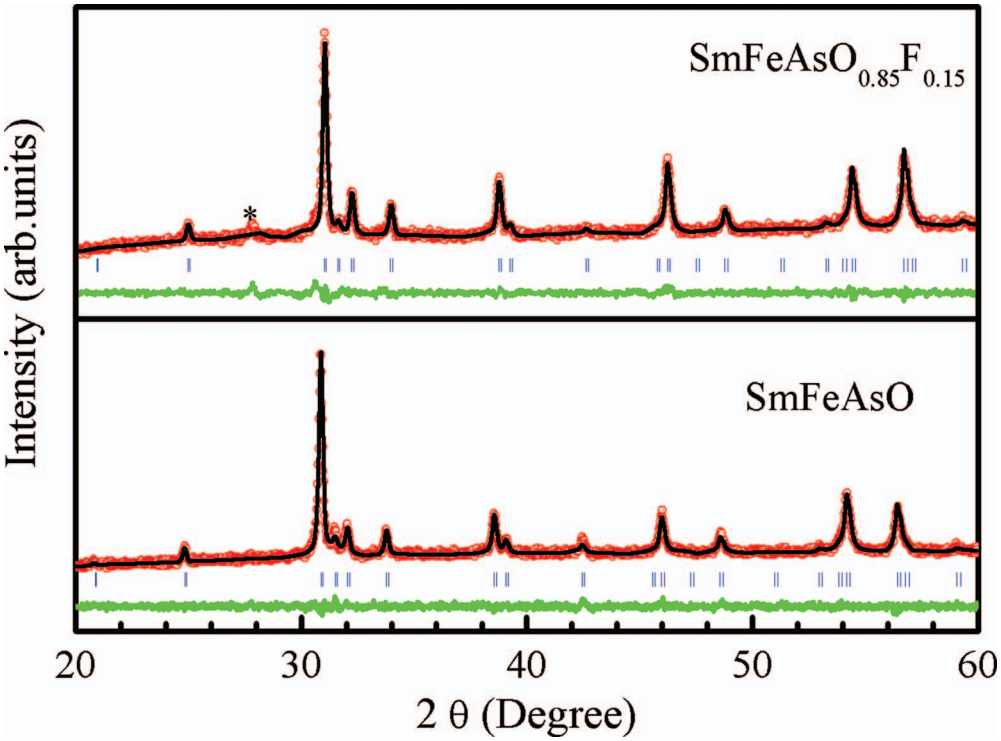

FIG. 1. Rietveld fitted room temperature *X*-ray diffraction patterns of SmFeAsO and $SmFeAsO_{0.85}F_{0.15}$. All the permitted diffraction planes are marked with blue vertical lines. The green line in the bottom shows the difference between the observed, Y^{obs} (red open circle) and fitted, Y^{calc} (black line) patterns (Y^{obs}- Y^{calc}).

of the grains in this sample. A typical example of this observation is presented in Fig. 2(b), the average thickness of the grain boundary in the present sample is ∼5 nm. The corresponding *SAED* pattern is shown in Fig. 2(c), which confirms the proper phase formation of $SmFeAsO_{0.85}F_{0.15}$. Evidence of a similar amorphous layer was also observed in polycrystalline $Sr_{0.6}K_{0.4}Fe_2As_2$ and $YBa_2Cu_3O_7$.[19,20] Generally, this amorphous layer results in the formation of weak link type grain boundaries (*GBs*) which in turn are detrimental to the intergrain current transport. Some reports have also suggested that most of the *GBs* of iron-based superconductors are indeed weak link type[20,21] and generally resemble to *GBs* in the layered cuprate superconductors. The presence of weak links and the corresponding weakly pinned inter-granular Josephson vortices are responsible for the thermally activated flux flow (*TAFF*) resistivity, which leads to both low J_c and the Arrhenius temperature dependence of resistivity.

Fig. 3(a) shows the temperature dependence of resistivity for SmFeAsO and $SmFeAsO_{0.85}F_{0.15}$ samples. The resistivity-temperature (ρ - T) curve of undoped SmFeAsO sample exhibits a sudden decrease at $T_{anomaly}$ ∼150 K. The anomaly apparent in the resistivity is known to be due to the collective effect of a crystallographic phase transition from the tetragonal *P*4/*nmm* to the orthorhombic *Cmma* space group around T∼150 K, and the occurrence of static spin density wave (*SDW*) instability like magnetic ordering of the Fe spins at a slightly lower temperature of ∼140 K.[5,7,12–18] The resistivity behaviour of SmFeAsO is semiconducting above 150 K and step like metallic at lower temperatures. After substitution of 15% O^{2-} by F^{1-}, the resistivity decreases monotonously with decreasing temperature. This decrease in resistivity suggests that the charge carrier density increases and the anomaly completely disappears with a concomitant appearance of superconductivity at below around T_c ($\rho = 0$) ∼55 K .Thus, the ρ - T curve of $SmFeAsO_{0.85}F_{0.15}$ shows the typical metallic behaviour till the superconducting transition is arrived at. The superconducting transition width, ΔT_c ($T_c^{onset} - T_c^{\rho=0}$), is found to be $\Delta T_c \sim 3.1$ K. The value of resistivity changes from 15.07 mΩ-cm at T∼300 K to 2.7 mΩ-cm just above the transition temperature. So the residual resistivity ratio (*RRR*)

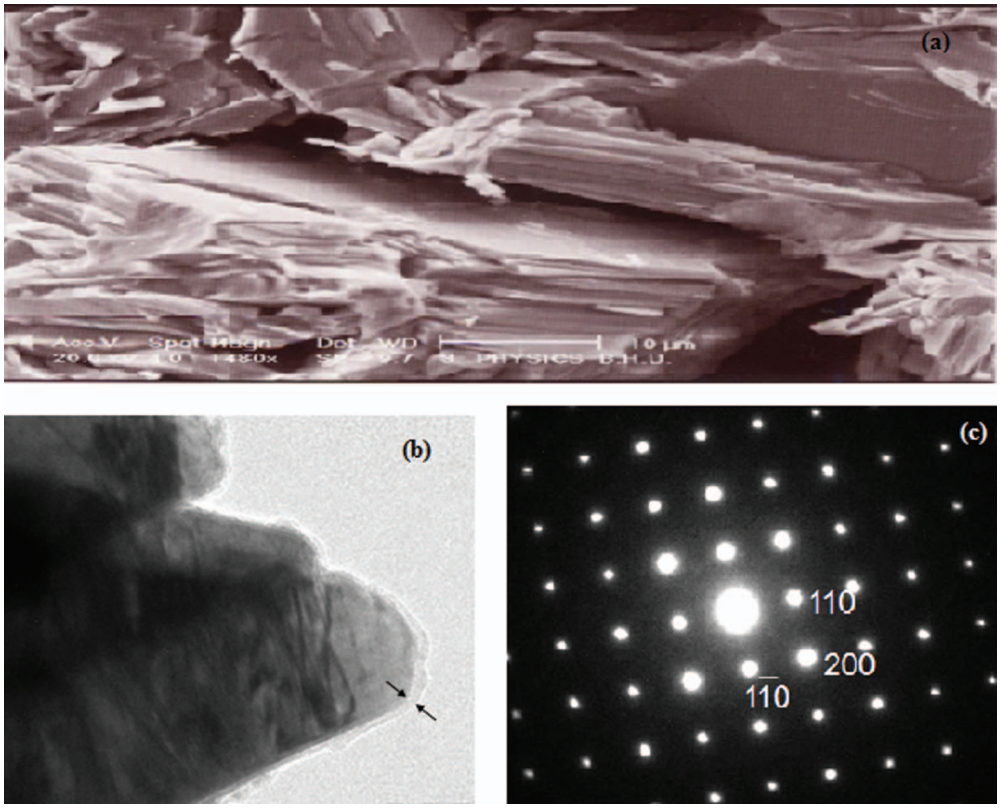

FIG. 2. (a) SEM, (b) TEM and (c) ED micrographs of studied 55 K superconducting $SmFeAsO_{0.85}F_{0.15}$ sample

for our studied $SmFeAsO_{0.85}F_{0.15}$ sample is 5.58, suggests good metallic normal-state connectivity. The broad transition is quite similar to what has been seen in a SmFeAsOF sample synthesized by two-step method. We would like to mention that the observed $T_c \sim 55$ K of our F-substituted ($SmFeAsO_{0.85}F_{0.15}$) sample is to the best our knowledge the highest for bulk samples prepared by a low temperature, two-step solid state reaction route and also without employing *HPHT*. $T_c \geq 55$ K has been reported previously but only in materials synthesized through *HPHT*.[8,17] The normal state resistivity above superconducting transition for the studied $SmFeAsO_{0.85}F_{0.15}$ sample shows linear dependence on temperature. The blue solid line in Fig. 3(a) shows the fitted resistance plot according to equation $\rho = \rho_0 + AT$, where ρ_0 is the residual resistivity and A is the slope of the graph. The experimental data fits well in the low temperature range. The linear behaviour of resistivity with temperature deviates above $T \sim 250$ K. The values of ρ_0 and A are found to be as 2.28 $\times$ 10^{-7} mΩ-cm and 5.19 $\times$ 10^{-8} mΩ-cm/K respectively. This behaviour is quite different from those shown by MgB_2[22] and other high-T_c superconductors.[23]

To obtain information about upper critical field Hc_2 and the flux pinning properties the temperature dependence of electrical resistivity under applied magnetic field [ρ (T, H)] from 0 to 130 kOe for superconducting $SmFeAsO_{0.85}F_{0.15}$ sample in the superconducting range has been measured and shown in Fig. 3(b). The resistive transition at $H = 0$ gets significant broadening in the applied magnetic field and is observed to become broader with the increasing H. This is generally regarded as a signature of strong vortex motion. This transition broadening with increasing magnetic field H, is a characteristic of type-II superconductors, especially the layered high T_c cuprate materials.[23] Further, it is interesting to note that the onset transition temperature (T_c^{onset}) remains nearly invariant with respect to H, the T_c ($\rho = 0$) is observed to decrease from $\sim$ 52 K to $\sim$42 K at $H = 130$ kOe. This could be due to the granular nature of the studied polycrystalline material, which promotes flux creep behaviour. The lowering of T_c ($\rho = 0$) with increasing H may be regarded as the coupled effect of the weal linked nature of the *GB*s and the vortex flow behaviour. The rate of decrease of

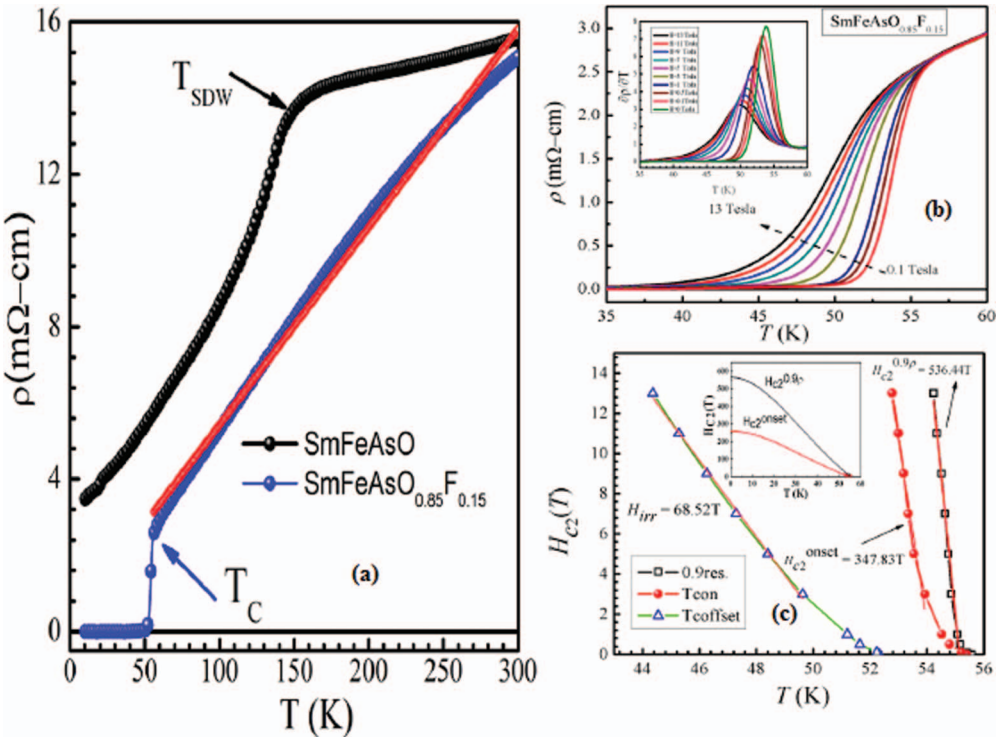

FIG. 3. (a) Temperature dependence of the resistivity $\rho(T)$ of SmFeAsO and $SmFeAsO_{0.85}F_{0.15}$ samples. Black arrow shows the anomaly temperature (T_m) for SmFeAsO and red arrow shows the superconducting transition temperature of doped sample. Solid blue line shows the linear fitted data in normal state for $SmFeAsO_{0.85}F_{0.15}$, (b) Resistivity behaviour under applied magnetic field $\rho(T)H$, up to 13Tesla for $SmFeAsO_{0.85}F_{0.15}$. Inset shows the derivates of resistivity for $SmFeAsO_{0.85}F_{0.15}$ in transition region and **(c)** Dependence of Upper critical field $H_{c2}(T)$ with temperature for 90% and 10 % drop of resistance of the normal state resistance and at onset (T_c ^{onset}). The inset shows estimation of $H_{c2}(T)$ for 90% drop of resistance of the normal state resistance and at onset (T_c ^{onset}) using the G-L approach.

transition temperature with applied magnetic field dT_c/dH ~0.8 K/T, which is appreciably smaller than the values measured for high T_c superconductor like, YBCO (dT_c/dH ~ 4 K/T, ref. 23) and MgB_2 (dT_c/dH ~ 2 K/T, ref. 22). This suggests a high value of upper critical field (H_{c2}) in these compounds. The upper critical field, H_{c2}, defined as the field at which the resistivity increases and approaches to the normal state resistivity, is an important parameter for evaluating the suitability of superconductor for high current/field application. The upper critical field Hc_2 has been evaluated by applying the criterion of 90% of normal resistivity at the onset temperature and by using a single-band Werthamer–Helfand–Hohenberg (*WHH*) model.[24] The experimental and the fitted values of the H_{c2} are presented in Fig. 3(c). The slope dHc_2/dT for 90% ρ_n is estimated to be −13.93T/K. Similarly the slope dH_{c2}/dT for 10% ρ_n is −1.89T/K at $T \leq 52$ K. The relation between dH_{c2}/dT and $H_{c2}(0)$ is defined by Werthamer–Helfand–Hohenberg (*WHH*) model as: $H_{c2}(0) = -0.693T_c(dH_{c2}/dT)T_c$. Thus estimated value of the upper critical fields are $H_{c2}(0)$ ~536T and ~68T for the 90% and 10% ρ_n fields, respectively and H_{irr} ~68.5T by the aforementioned model. The extrapolated lines in the inset of Fig. 3(c) are drawn by using the Ginzburg–Landau equation $H_{c2}(T) = H_{c2}(0)$ $(1 - t^2)/(1 + t^2)$ where $t = T/T_c$ is the reduced temperature and $H_{c2}(0)$ is the upper critical field for 90% ρ_n at zero temperature which gives H_{c2} as ~565.80T, which is slightly higher than that estimated by *WHH* approach. Assuming $H_{c2}(0) = H_{c2}(WHH_0)$, the Ginzburg–Landau coherence length $\xi_{GL} = (\Phi_0/2\pi H_{c2})^{1/2}$, where $\Phi_0 = 2.07 \times 10^{-7}$ G cm^2 yields zero temperature coherence length $\xi_{GL}(0)$ ~ 7.8 Å which is clearly smaller than the repeat distance of FeAs layer of d = 8.5 Å, therefore at low temperature 2D superconducting behaviour is expected. These estimated values of H_{c2} clearly demonstrate the robustness of the present ~55 K superconducting $SmFeAsO_{0.85}F_{0.15}$ against the applied magnetic field. The above estimations are only suitable for the one-band case. However, in this

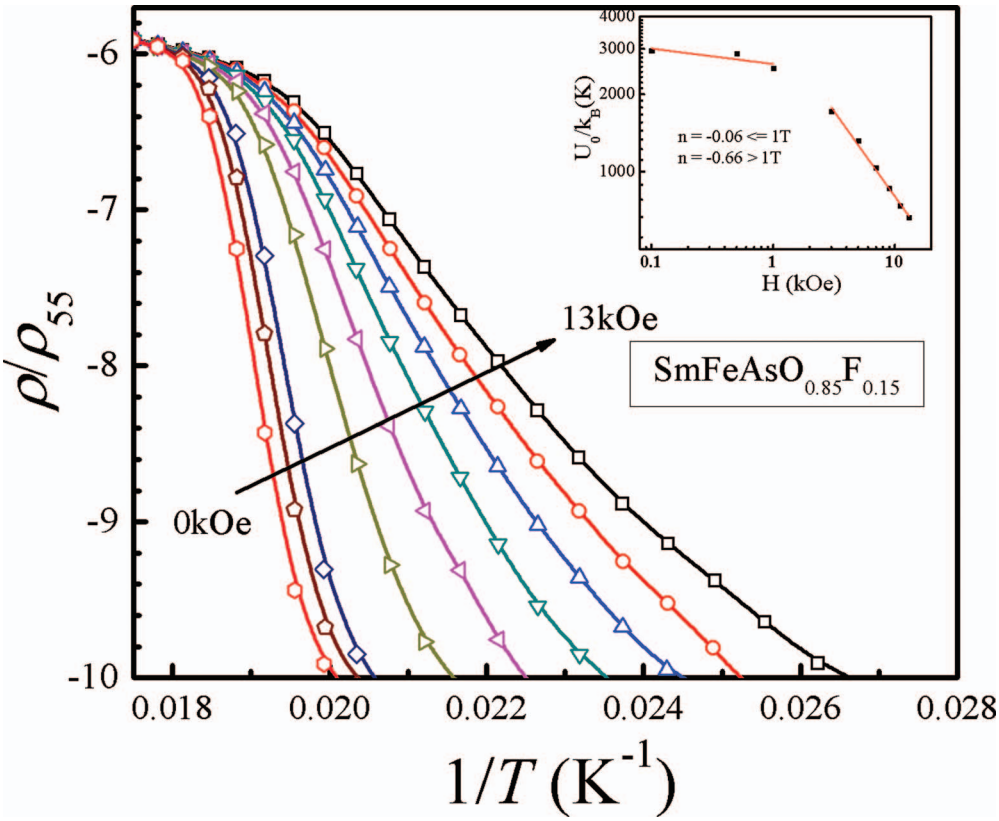

FIG. 4. The Arrhenius plot of resistivity at different field to study the thermally activation flux flow for $smFeAsO_{0.85}F_{0.15}$ sample. Inset show the magnetic field dependence of *TAFF* activation energy (U_0).

new type of superconductor, the band structure calculation indicates the existence of multiple bands across the Fermi levels. As our analysis neglects multiple band effect, the real upper critical fields in the present system could be very high upper critical field suggests a very prospective application of this superconducting envisaged material.

The temperature derivative of resistivity for the superconducting $SmFeAsO_{0.85}F_{0.15}$ sample at various applied fields has been shown in inset of Fig. 3(d). The $d\rho/dT$ shows a narrow intense maxima centred at superconducting transition temperature in zero applied fields, which indicate good percolation path of superconducting grains. The broadening of the $d\rho/dT$ peak increases with applied magnetic field. The broad peak at low temperatures range indicates the intra-grain and inter-grain regimes.[23] It is interesting to note that a clear second peak in $d\rho/dT$, usually observed in case of the high T_c cuprate materials,[23] is absent in the presently studied $SmFeAsO_{0.85}F_{0.15}$. This suggests that unlike the insulating *GB*s between superconducting grains in the high T_c cuprate materials, the same are mostly metallic in the case of $SmFeAsO_{0.85}F_{0.15}$. On the other hand, the broadening in $d\rho/dT$ peak with applied field, suggestive of weaker inter granular coupling, is relatively higher for $SmFeAsO_{0.85}F_{0.15}$ than for MgB_2.[22]

The broadening of resistive transition in applied magnetic field is due to the creep of vortices and as a result the dependence is thermally activated. The temperature dependence of resistivity in the broadened region is generally described by Arrhenius equation $\rho(T,B) = \rho_0 \exp[-Uo/k_BT]$, ρ_0 is the field independent pre-exponential factor (here normal state resistance at 55 K(ρ_{55}) is taken as ρ_0) and k_B is Boltzmann's constant and U_0, the flux-flow activation energy which can be obtained from the slope of the linear part of an Arrhenius plot.[25,26] The Arrhenius plot of $\rho(T)$ shows linearity in limited temperature interval below T_c, the activation energy U_0 can be deduced from this region. The Arrhenius plots of $\rho(T)$ for superconducting $SmFeAsO_{0.85}F_{0.15}$ sample in applied fields of up to 130 kOe are presented in Fig. 4. The best fitted experimental data gives the value of activation energy

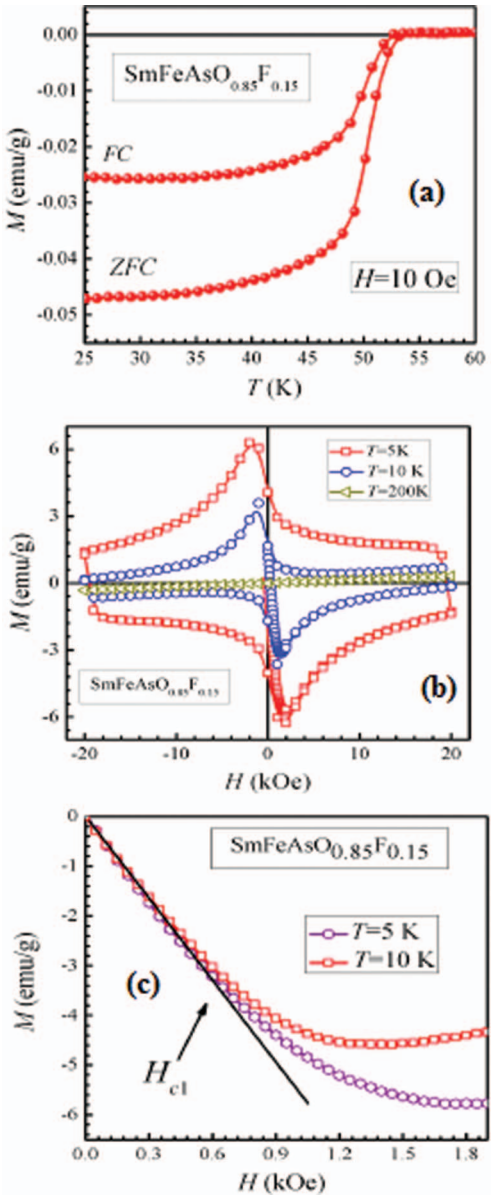

FIG. 5. (a) Temperature dependence *DC* magnetic susceptibility $M(T)$ in both *ZFC* and *FC* situation of $SmFeAsO_{0.85}F_{0.15}$ sample under applied field of 10Oe, (b) Variation of Magnetization under applied magnetic field, $M(H)$ at 5K, 10 K and 200 K of $SmFeAsO_{0.85}F_{0.15}$ sample and (c) The Lower critical field (H_{c1}) at 5 and 10 K for the superconducting $SmFeAsO_{0.85}F_{0.15}$ sample

(U_0/k_B) ranging from 2961 K and 662 K in fields of 0.1 kOe and 130 kOe, respectively. The activation energy shows different power law dependence on applied magnetic field.[27] In the present study, the activation energy shows weak field dependence i.e. $U_0/k_B \sim H^{-0.06}$ at small magnetic field ($H < 10$ kOe). However, at higher values of H, the field dependence is much stronger; $U_0/k_B \sim H^{-0.66}$. Inset of Fig. 4 depicts the magnetic field dependence (up to 130 kOe) of the activation energy U_0/k_B for $SmFeAsO_{0.85}F_{0.15}$ sample. These values are in good agreement with previous reports.[12,27]

To understand the magnetic behaviour comprehensively the temperature and field dependent magnetization measurements have been carried out. Fig. 5(a) shows the temperature dependence of the *DC* magnetization of the $SmFeAsO_{0.85}F_{0.15}$ sample measured under zero field cooled (*ZFC*) and field cooled (*FC*) measuring conditions at $H = 10$ Oe. The negative susceptibility in both *ZFC*

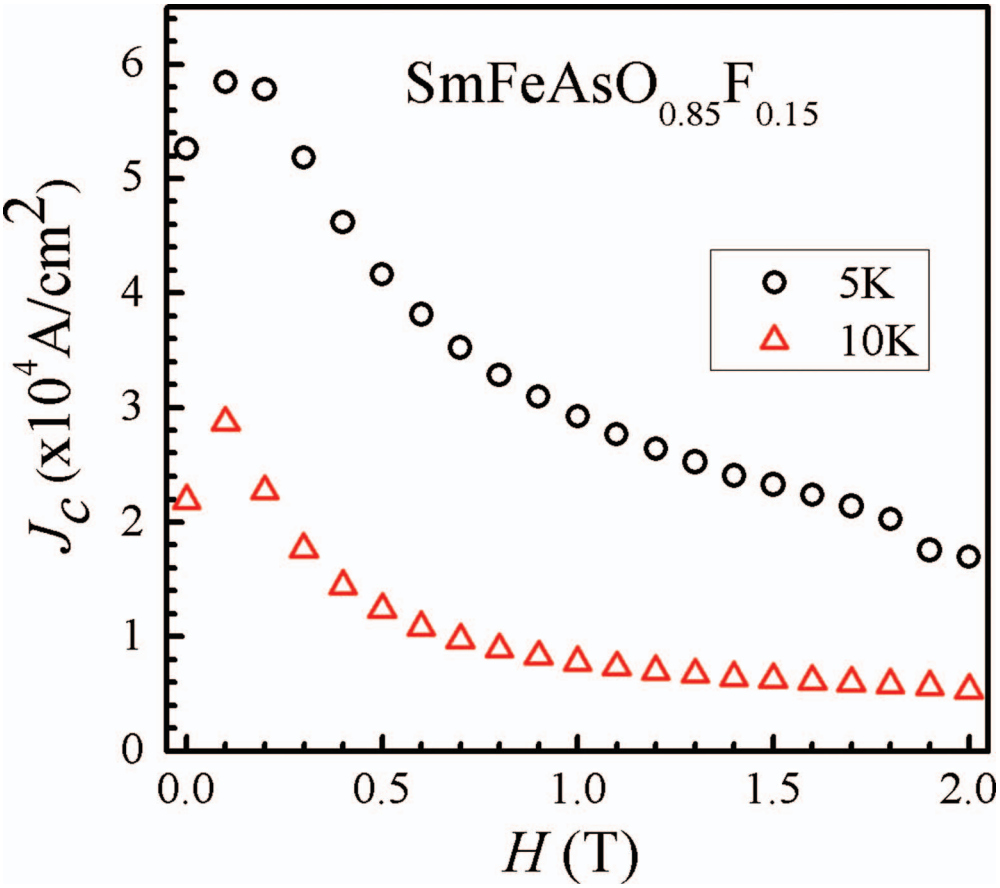

FIG. 6. The Variation of Critical current density (J_c) with applied magnetic field.

and *FC* condition confirm the bulk superconductivity. The susceptibility signal becomes negative below 54 K. This indicates that bulk superconductivity sets below this temperature. Both *ZFC* and *FC* curves are nearly saturated below 45 K. The minute difference in T_c (onset) obtained from resistivity $\rho(T)$ and magnetization $M(T)$ is due to the threshold for transport measurements. The transport measurement is through percolation path and hence is lower in comparison to bulk diamagnetic response. The difference in *ZFC* and *FC* curves of the sample also suggests that the material has a fairly large flux pinning force resulting in the trapping of magnetic flux under the field cooling condition. Fig. 5(b) depicts the isothermal magnetization $M(H)$ loops of the superconducting $SmFeAsO_{0.85}F_{0.15}$ sample at 5 K, 10 K and 200 K, with applied fields of up to 20 kOe. The M (H) loops are wide open at 5 K and 10 K up to 20 kOe and thus confirming the bulk superconductivity in the studied sample. The lower critical field (H_{c1}) i.e. the characteristic value at which the applied magnetic field starts to penetrate the sample has been deducted from the $M(H)$ loops. The magnetic field, at which the magnetization deviates from the linearity, is also defined as lower critical field of superconducting materials. The variation of Magnetization under applied magnetic field, M (H) plots for the $SmFeAsO_{0.85}F_{0.15}$ sample at temperature 5 K and 10 K are shown in the Fig. 5(c). The lower critical field deducted from the graph is found to be $H_{c1} \sim$ 650 Oe at 5 K and 10 K.

Fig. 6 shows the magnetic field dependence of the critical current density J_c being derived from the hysteresis loop (MH) width using the extended Bean critical state model $J_c = 20\Delta M/\text{Va}(1 - \text{a}/3\text{b})$, where ΔM is the height of the magnetization loop measured in emu, V is the volume of the sample in cm^3, a and b are the respective sample dimensions in cm and J_c is in Acm^{-2}. For estimation of J_c, the full sample dimensions of 7.1 × 2.62 × 2.28 mm^3 were taken. At 5 K, the J_c is found to be approximately 5.26×10^4 cm^{-2} at $H = 0$ which decreases to $2.2 \times 10^3 Acm^{-2}$ at H = 100 kOe. It can also be observed from Fig. 6 that J_c at 5 K decreases rapidly up to

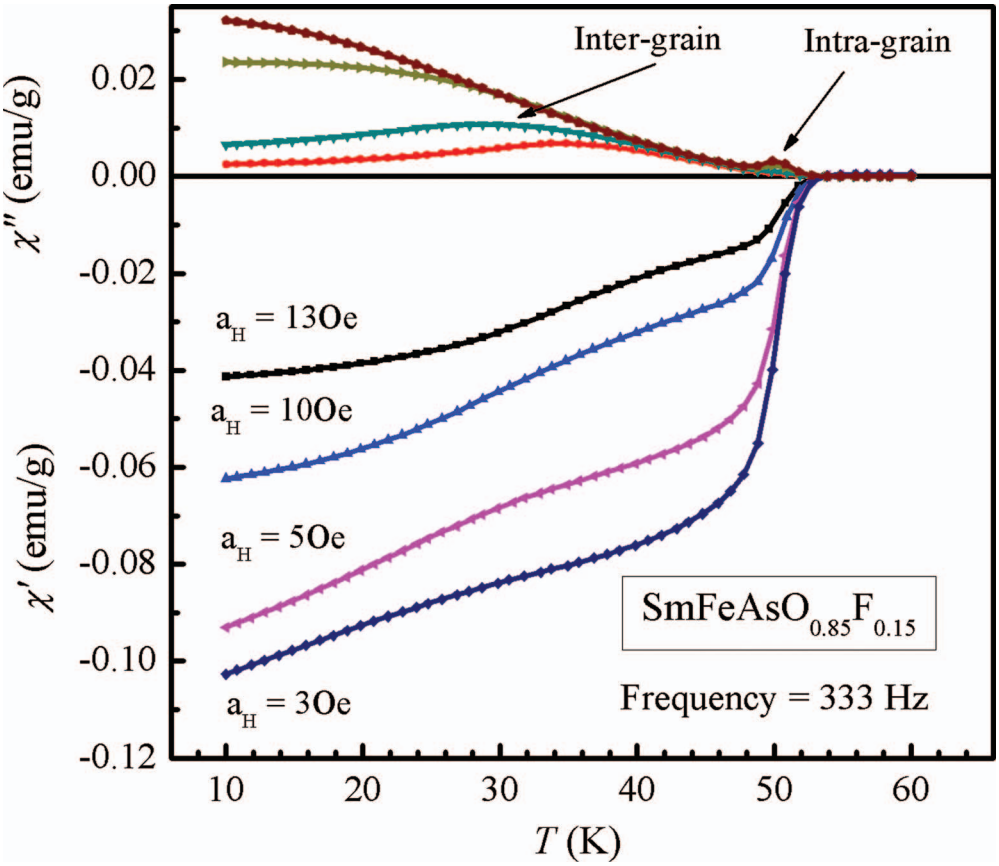

FIG. 7. The real (χ') and imaginary ($i\chi''$) components of *AC* susceptibility as function of temperature measured at various *AC* drive field, ranging from 3Oe to 13Oe at 333*Hz* for $SmFeAsO_{0.85}F_{0.15}$ sample.

$H = 20$ kOe. These values of J_c are found to be in good agreement with the reported results for the $SmFeAsO_{0.85}F_{0.15}$ superconductor.[28] However, J_c values of $SmFeAsO_{0.85}F_{0.15}$ superconductor at 5 K obtained is significantly lower than that of the MgB_2 bulk samples which generally attain 10^6 Acm^{-2} at 4.2 K. The possible reasons for lower value of J_c could be the presence of second minor impurity phase or the weak link nature of the *GB*s. Although the whole-sample current densities are significantly lower than that in randomly grain-oriented bulk of MgB_2, the grain connectivity seems to be better than that of random polycrystalline high T_c cuprates.

In order to understand granular nature of the superconducting sample and in particular to find out the intra and inter grain contributions at high temperatures, the ac susceptibility measurement for the superconducting sample at zero *DC* bias magnetic fields has been performed.[19,29,30] The real (χ') and imaginary ($i\chi''$) components of ac susceptibility as function of temperature measured at various *AC* drive field, ranging from 3Oe to 13Oe at fixed frequency f = 333 Hz are presented in Fig. 7. It is clear from the real part of the susceptibility (χ') that the diamagnetic onset transition temperature is same irrespective to the drive fields and in imaginary ($i\chi'$) components of ac susceptibility two peaks appear in which the higher temperature peak corresponds to the individual superconducting grains i.e. intra granular superconductivity whereas the lower temperatures peak corresponds to the intergranular coupling. The intergranular peak shifts towards lower temperature with increasing ac drive fields and gets broadened, due to the weak coupling between the grains.[31]

The temperature dependence of specific heat for the pure and doped samples is shown in Fig. 8. The absolute values of C_p are quite close for both the samples. A clear jump is observed in C_p data of SmFeAsO around the same temperature at which a metallic step has been seen (Fig. 2(a)) in resistivity measurements. This jump in SmFeAsO heat capacity around 140 K is due

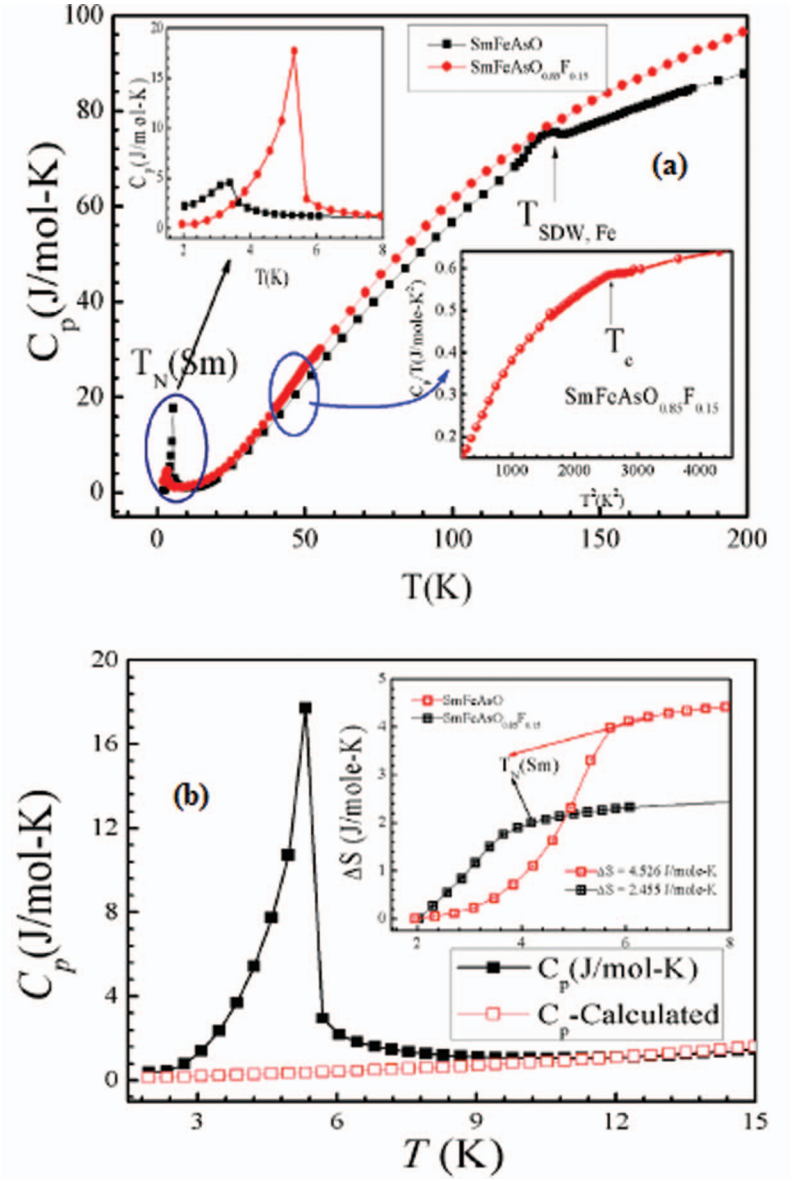

FIG. 8. (a) Specific heat of SmFeAsO and $SmFeAsO_{0.85}F_{0.15}$ sample (main panel). Inset shows enlarge view of the superconducting transition C_p/T Vs T^2 near T_c region and (b) Observed and fitted Specific heat of SmFeAsO near the *AFM* ordering of Sm spins, the inset shows that change in entropy near *AFM* ordering of Sm spins for both non superconducting (SmFeAsO) and superconducting ($SmFeAsO_{0.85}F_{0.15}$) samples.

to the spin density wave (*SDW*) character exhibited by the compound. Such jump in specific heat completely disappears in superconducting sample. Heat capacity decreases with further decrease in temperature and an additional peak is observed at 4.5 K which may be due to the antiferromagnetic ordering of Sm^{3+} ions. The lower inset of Fig. 7 shows measured value of C_p/T Vs T^2. At the superconducting transition temperature (T_c), a hump in the Cp/T Vs T^2 plot has been observed. The shape of the Lambda transition for superconducting $SmFeAsO_{0.85}F_{0.15}$ does not exhibit sharp discontinuity at T_c, as has been reported for other superconductors.[32,33] In general, the heat capacity of non superconducting SmFeAsO and superconducting $SmFeAsO_{0.85}F_{0.15}$ exhibits clearly the coupled *SDW*/structural phase transition at around 150 K for the former and a discontinuity in the Cp/T vs T^2 for the later at superconducting transition temperature of 55 K.

To elucidate the non-magnetic contribution of heat capacity and change in entropy for anti-ferromagntic (T_N) ordering of Sm^{3+} spins in non superconducting SmFeAsO and superconducting $SmFeAsO_{0.85}F_{0.15}$ samples, the polynomial interpolation method using equation $aT + bT^3$ has been used to fit the $Cp(T)$ plot of both samples.[10,34] The fitted and observed $C_P(T)$ are close to the T_N of Sm is shown in Fig. 8(b). Using the fitted value of the coefficients a and b, the data has been extrapolated to estimate the background contribution of heat capacity in the lower temperature range. In order to calculate the change in entropy, the change in specific heat (ΔC_P) is found by first subtracting the background contribution from the experimental data and further the integration over $\Delta C_P/T$ provides the entropy change ΔS. The integrated result (ΔS) provides the values ~4.256 J/mole-K and 2.455 J/mole-K for SmFeAsO and $SmFeAsO_{0.85}F_{0.15}$ superconducting samples, respectively. The change in entropy near T_N of Sm for both the samples is shown in inset of Fig. 8(b). It is interesting to note that change in entropy (ΔS) for T_N of Sm is reduced by over 40% for the superconducting ($SmFeAsO_{0.85}F_{0.15}$) sample in comparison to its non-superconducting (SmFeAsO) counter part.

IV. CONCLUSION

In summary, the structural, microstructural and magnetotransport properties of $SmFeAsO_{0.8}5F_{0.15}$ superconductor synthesized at low temperature by two-step low temperature solid state reaction process have been investigated. In this nearly single phase material, having weak link type *GB*s, the superconducting transition onsets at ~55 K and the zero field transition width is ~3 K. The *DC* magnetization and *AC* susceptibility measurement also provide clear evidence of weak link nature of the *GB*s. Our results show that despite the weak link nature of the *GB*s the decrement in T_c ($\rho = 0$) with magnetic field, $dT_c/dH \sim 0.8$ K/T is appreciably smaller than the high T_c cuprates. The observed broadening of resistive transition in applied magnetic field is caused by the creep of flux vortices and motion is thermally activated. At lower H, the activation energy shows weak field dependence, while at higher values it becomes much stronger. Although the J_c of our samples is moderate but the decay in it under H is comparatively smaller. We believe that more studies are required to further understand the nature of the *GB*s and its consequences on the magneto-transport properties.

ACKNOWLEDGMENT

The authors are thankful to Prof.Ratnamala Chatterjee (*IITD*). One of the authors (A.S.) would like to acknowledge *UGC*-India and Dr. U.P. Singh (Principal *TDPG* College) for providing Teacher fellowship award under *FIP*. The work at *CSIR-NPL* is financially supported by *DAE-SRC* outstanding investigator award scheme to work on search for new superconductors.

[1] Y. Kamihara, T. Watanabe, M. Hirano, and H. Hosono, J. Am. Chem. Soc. **130**, 3296 (2008).
[2] X. H. Chen, T. Wu, G. Wu, R. H. Liu, H. Chen, and D. F. Fang, Nature **453**, 761 (2008).
[3] Z. A. Ren, J. Yang, W. Lu, W. Yi, X. L. Shen, Z. C. Li, G. C. Che, X. L. Dong, L. L. Sun, F. Zhou, and Z. X. Zhao, Europhys. Lett. **82**, 57002 (2008).
[4] Z. A. Ren, J. Yang, W. Lu, W. Yi, G. C. Che, X. L. Dong, L. L. Sun, and Z. X. Zhao, Mater. Res. Innov. **12**, 1 (2008).
[5] G. F. Chen, Z. Li, D. Wu, G. Li, W. Z. Hu, J. Dong, P. Zheng, J. L. Luo, and N. L. Wang, Phys. Rev. Lett. **100**, 247002 (2008).
[6] T. Yildirim, Phys. Rev. Lett. **101**, 057010 (2008).
[7] L. J. Li, Y. K. Li, Z. Ren, Y. K. Luo, X. Lin, M. He, Q. Tao, Z. W. Zhu, G. H. Cao, and Z. A. Xu, Phys. Rev. B **78**, 132506 (2008).
[8] P. Cheng, L. Fang, H. Yang, X. Zhu, G. Mu, H. Luo, Z. Wang, and H. H. Wen, Sci. China **G51**, 719 (2008).
[9] V. P. S. Awana, R. S. Meena, A. Pal, A. Vajpayee, K. V. R. Rao, and H. Kishan, Eur. Phys. J. B **79**, 139 (2011).
[10] I. Nowik, I. Felner, V. P. S. Awana, Arpita Vajpayee, and H. Kishan, J. Phys. Cond. Matt. Fast Track Commun. **20**, 292201 (2008).
[11] V. P. S. Awana, Arpita Vajpayee, Anand Pal, Monika Mudgel, R. S. Meena, and H. Kishan, J Supercond Nov Magn **22**, 623 (2009).
[12] Anand Pal, S. S. Mehdi, Mushahid Husain, and V. P. S. Awana, Solid State Sciences **15**, 123 (2013).
[13] A. Narduzzo, M. S. Grbić, M. Požek, A. Dulčić, D. Paar, A. Kondrat, C. Hess, I. Hellmann, R. Klingeler, J. Werner, A. Köhler, G. Behr, and B. Büchner, Phys. Rev. B **78**, 012507 (2008).
[14] F. Hunte, J. Jaroszynski, A. Gurevich, D. C. Larbalestier, A. S. Jin, R. Sefat, M. A. McGuire, B. C. Sales, D. K. Christen, and D. Mandrus, Nature **453**, 903 (2008).

[15] C. Senatore, R. Flukiger, M. Cantoni, G. Wu, R. H. Liu, and X. H. Chen, Phys. Rev. B **78**, 054514 (2008).
[16] X. L. Wang, S. R. Ghorbani, G. Peleckis, and S. X. Dou, Adv. Mater. **21**, 236 (2008).
[17] R. Zhi-An, L. Wei, Y. Jie, Y. Wei, S. X. Li, Z. Cai, C. G. Can, D. X. Li, S. L. Ling, Z. Fang, and Z. Z. Xian, Chinese Phys. Lett. **25**, 2215 (2008).
[18] M. Tropeano, C. Fanciulli, C. Ferdeghini, D. Marrè, A. S. Siri, M. Putti, A. Martinelli, M. Ferretti, A. Palenzona, M. R. Cimberle, C. Mirri, S. Lupi, R. Sopracase, P. Calvani, and A. Perucchi, Super. Sci. & Technol. **25**, 034004 (2009).
[19] L. Wang, Y. Qi, D. Wang, X. Zhang, and Y. Ma, Superconductor Sci. and Tech. **23**, 025027 (2010).
[20] Y. Matsumoto, J. Hombo, and Y. Yamaguchi, Appl. Phys. Lett. **56**, 1585 (1990).
[21] J. H. Durell, C.-B Eom, A. Gurvich, E. E. Hellstrom, C. Tarantini, and D. C. Larbalestier, Rep. Prog. Phys. **74**, 124511 (2011).
[22] V. P. S. Awana, Arpita Vajpayee, Monika Mudgel, V. Ganesan, A. M. Awasthi, G. L. Bhalla, and H. Kishan, Eur. Phys. J. B **62**, 281 (2008).
[23] N. P. Liyanawaduge, S. K. Singh, A. Kumar, R. Jha, B. S. B. Karunarathne, and V. P. S. Awana, Supercond. Sci. Technol. **25**, 035017 (2012).
[24] E. Helfand and N. R. Werthamer, Phys. Rev. **147**, 288 (1966).
[25] A. Gurevich, Rep. Prog. Phys. **74**, 124501 (2011).
[26] J. J. Jaroszynski, F. Hunte, L. Balicas, Jo Youn-jung, I. Rai Cevic, A. Gurevich, D. C. Larbalestier, F. F. Balakirev, L. Fang, P. Cheng, Y. Jia, and H. H. Wen, Phys. Rev. B **78**, 174523 (2008).
[27] C. Shekhar, Amit Srivastava, Pramod Kumar, Pankaj Srivastava, and O. N. Srivastava, Supercond. Sci. Technol. **25**, 045004 (2012).
[28] L. Wang, Z. Gao, Y. Qi, X. Zhang, D. Wang, and Y. Ma, Supercond. Sci. Technol. **22**, 015019 (2009).
[29] M. Nikolo and R. B. Goldfarb, Phys. Rev. B **39**, 6615 (1989).
[30] G. Bonsignore, A. Agliolo Gallitto, M. Li Vigni, J. L. Luo, G. F. Chen, N. L. Wang, and D. V. Shovkun, J. Low. Temp. Phys. **162**, 40 (2011).
[31] A. Agliolo Gallitto, G. Bonsignore, M. Bonura, and M. L. Vigni, J. Phys. Conf. Series **234**, 012001 (2010).
[32] L. Ding, C. He, J. K. Dong, T. Wu, R. H. Liu, X. H. Chen, and S. Y. Li, Phys. Rev. B **77**, 180510 (2008).
[33] M. Tropeano, A. Martinelli, A. Palenzona, E. Bellingeri, E. Galleani d'Agliano, T. D. Nguyen, M. Affronte, and M. Putti, Phys. Rev. B **78**, 094518 (2008).
[34] V. P. S. Awana, Anand Pal, M. Husain, and H. Kishan, J Supercond Nov Magn **24**, 151 (2011).